



## Strontium isotopes and cremation: Investigating mobility patterns in the Roman city of *Mutina* (north-eastern Italy)

Francesca Seghi<sup>a,\*</sup>, Federico Lugli<sup>b,c</sup>, Hannah F. James<sup>d</sup>, Tessi Löffelmann<sup>d,e</sup>,  
Elena Armaroli<sup>b</sup>, Antonino Vazzana<sup>a</sup>, Anna Cipriani<sup>b</sup>, Christophe Snoeck<sup>d</sup>, Stefano Benazzi<sup>a</sup>

<sup>a</sup> Department of Cultural Heritage, University of Bologna, Via degli Ariani 1, Ravenna 48121, Italy

<sup>b</sup> Department of Chemical and Geological Sciences, University of Modena and Reggio Emilia, Via Giuseppe Campi 103, Modena 41125, Italy

<sup>c</sup> Institut für Geowissenschaften, Goethe University Frankfurt, Altenhöferallee 1, Frankfurt am Main 60438, Germany

<sup>d</sup> Archaeology, Environmental Changes and Geo-Chemistry, Vrije Universiteit Brussel, Pleinlaan 2, Brussels 1050, Belgium

<sup>e</sup> Department of Archaeology, Durham University, South Road, Durham DH1 3LE, United Kingdom

### ARTICLE INFO

#### Keywords:

Cremation  
Isotopes  
Mobility  
Roman Empire  
*Mutina*

### ABSTRACT

Cremation was a very common ritual in ancient Roman funerary traditions. However, the study of cremated human remains has always been complex and challenging, which has often led to an imbalance in data recording between inhumations and cremations. In this work, we study 14 cremation burials from two different urban cemeteries in the Roman city of *Mutina* (Modena, Emilia-Romagna, north-eastern Italy). The use of strontium isotope analysis provides insights into the mobility pattern and provenance of individuals cremated and buried at *Mutina*. The isotopic results suggest that nine samples fall outside the local bioavailable strontium range of the city of Modena, given their different  $^{87}\text{Sr}/^{86}\text{Sr}$  values compared to the ratio compatible with alluvial deposits in the Po Valley. Both the isotopic results and the manufacture of some funerary objects suggest that the probable provenance of some individuals is compatible with western (Pre)Alpine areas. The values of  $^{87}\text{Sr}/^{86}\text{Sr}$  also complement the results obtained from the osteological analysis increasing the minimum number of individuals buried in at least one grave. Our study revealed key insights about cremated individuals from Italy, highlighting variations of the mobility patterns within Roman funerary contexts of *Mutina*.

### 1. Introduction

Cremation was a common practice in ancient Rome and was interpreted as a means of purification aimed at freeing the soul and facilitating its entry into the afterlife (McKinley, 1994; Schmidt and Symes, 2015). The ritual was divided into two categories: cremations with the use of the “*bustum*” (i.e., a pit in the ground that had first the function of hosting the funeral pyre and then that of final burial, collecting the ashes of the individual) and cremations known as “*ustrinum*”, where there was a separation between the environment in which the incineration of the body took place, and the actual burial place. Ashes and burnt bones were then placed inside urns and then deposited in pits (Noy, 2000; Rottoli and Castiglioni, 2011). Evidence indicates that cremation practices could vary according to social status, family preferences and cultural influences (Schmidt and Symes, 2015).

Exposure of bones and teeth to high temperatures represents a peculiar taphonomic process (Efremov, 1940). Skeletal elements undergo numerous changes both macroscopically and microscopically. Regarding macroscopic modifications, burnt bones and teeth show changes in appearance (e.g., colour) and size (Enzo et al., 2007; Thompson et al., 2017; Walker et al., 2008). Loss of the organic component and dehydration, in fact, cause fractures to form (i.e., U-shaped fractures along the diaphysis of long bones), and lead to significant shrinkage of skeletal elements (Shipman et al., 1984; Thompson, 2005). Microscopically, high temperatures cause degradation of organic matter and a reorganization of the inorganic component: bioapatite crystals change in size and arrange themselves into a more ordered crystalline matrix (Snoeck et al., 2014; Thompson et al., 2017).

All of this makes cremated human remains a source of debate and controversy. Their highly fragmentary nature makes anatomical

\* Corresponding author.

E-mail addresses: [francesca.seghi2@unibo.it](mailto:francesca.seghi2@unibo.it) (F. Seghi), [federico.lugli@unimore.it](mailto:federico.lugli@unimore.it) (F. Lugli), [hannah.james@vub.be](mailto:hannah.james@vub.be) (H.F. James), [tessi.loeffelmann@vub.be](mailto:tessi.loeffelmann@vub.be) (T. Löffelmann), [elena.armaroli@unimore.it](mailto:elena.armaroli@unimore.it) (E. Armaroli), [antonino.vazzana2@unibo.it](mailto:antonino.vazzana2@unibo.it) (A. Vazzana), [anna.cipriani@unimore.it](mailto:anna.cipriani@unimore.it) (A. Cipriani), [christophe.snoeck@vub.be](mailto:christophe.snoeck@vub.be) (C. Snoeck), [stefano.benazzi@unibo.it](mailto:stefano.benazzi@unibo.it) (S. Benazzi).

<https://doi.org/10.1016/j.jasrep.2024.104728>

Received 11 April 2024; Received in revised form 28 June 2024; Accepted 12 August 2024

Available online 21 August 2024

2352-409X/© 2024 The Authors. Published by Elsevier Ltd. This is an open access article under the CC BY-NC-ND license (<http://creativecommons.org/licenses/by-nc-nd/4.0/>).

recognition and assessment of the biological profile (e.g., estimation of sex and age-at-death, evaluation of pathology) challenging. The difficulty in analysing this material arises during the archaeological excavation and persists in later stages, especially when the remains are assessed in the laboratory (Thompson et al., 2017; Williams, 2008).

However, it has been shown that calcined bones (i.e., when the degree of combustion reaches a temperature above 600 °C; Zazzo et al., 2013) are resistant to post-mortem diagenetic processes, providing a reliable substrate for strontium isotope analysis for the investigation of mobility patterns, once adequate pre-treatment has been carried out (McMillan et al., 2019; Snoeck et al., 2015). Indeed, as mentioned above, high temperature can alter not only the colour of the cortical and trabecular bone tissue (Walker et al., 2008), but also the mineral structure of the bone, which loses organic matter and becomes more crystalline (Person, 1995; Snoeck et al., 2014; Surovell and Stiner, 2001; Van Strydonck et al., 2010), limiting a post-mortem alteration of the biogenic chemical signal.

In our study, we conducted a comprehensive analysis of the cremations unearthed from two Roman funerary contexts. We integrated osteological examinations to delineate the biological profile of the individuals and strontium isotope analysis to investigate their mobility patterns, while also integrating an evaluation of grave goods to add contextual information to better clarify these patterns.

### 1.1. Strontium isotopes

Strontium is a chemical element that belongs to the alkaline earth metal group. In nature, it exists in the form of four isotopes:  $^{84}\text{Sr}$ ,  $^{86}\text{Sr}$ ,  $^{87}\text{Sr}$  and  $^{88}\text{Sr}$ .  $^{84}\text{Sr}$ ,  $^{86}\text{Sr}$  and  $^{88}\text{Sr}$  are non-radiogenic, while  $^{87}\text{Sr}$  forms through the decay of rubidium ( $^{87}\text{Rb}$ ). The half-life is  $4.88 \times 10^{10}$  years (Faure and Mensing, 2005).

Through the bedrock erosion, strontium isotopes enter the soil mixing with groundwater, surface water and atmospheric precipitation, also reaching the oceans and thus integrating into the local ecosystem. Bioavailable strontium is absorbed by plants through the roots and by animals through diet and drinking water, replacing calcium in the biapatite of skeletal tissues (bones and teeth; Bentley, 2006). These properties make  $^{87}\text{Sr}$  and  $^{86}\text{Sr}$  isotopes, and especially their ratio, a geological marker for tracing the geographical origins of biological materials (Faure and Powell, 1972).

### 1.2. Archaeological context of Mutina

Mutina, known today as the city of Modena (Emilia Romagna, north-eastern Italy), was an important commercial and political centre in the north of the peninsula during the Roman Empire, thanks to its strategic location along the *Via Aemilia* (Pellegriani, 2017). Numerous burial spaces have been discovered in the city, located close to residential areas, demonstrating the proximity between the spaces dedicated to funeral rites and the communities that lived there. As far as funerary rituals are concerned, cremation was the most widely used rite until the 1<sup>st</sup> century CE in Mutina, with only sporadic inhumations from the second half of this century (Ortalli, 2017; Pellegriani, 2017). From the 2<sup>nd</sup> century CE onwards, and especially from the 3<sup>rd</sup> and 4<sup>th</sup> centuries CE, cremations gradually declined being replaced by inhumation, which became the predominant funeral rite (Ortalli, 2017; Pellegriani, 2017). Over the past 30 years, numerous excavations have been conducted, uncovering around 300 burials, both from the Roman and Late Antique periods.

Among the burial spaces, the necropoleis of Via Emilia Est-Via Cesana and Via Emilia-Tangenziale Pasternak are two of the most investigated, and both include tombs dated from the 1<sup>st</sup> century BCE to the 2<sup>nd</sup> century CE (Ortalli, 2017). The Via Emilia Est-Via Cesana is an urban necropolis which was excavated between 2004 and 2005 and contained a total of 29 cremation burials (Fig. 1). It went through different phases of occupation: at the beginning, the necropolis was only sporadically used, but there was already a definite occupation of the space; in the Julio-Claudian period (2<sup>nd</sup> century CE) the area was characterised by a period of maximum exploitation, followed by a gradual abandonment in the late imperial phase. The only inhumation in the necropolis is dated to the Late Antique period (5<sup>th</sup>-6<sup>th</sup> century CE; Ortalli, 2017). In 2007, the urban necropolis of the Via Emilia-Tangenziale Pasternak was excavated and yielded a total of 15 cremations (no inhumations were present in this necropolis). It was abandoned after the 2<sup>nd</sup> century CE. For both necropoleis, except for rare cases of direct cremations, most of the burials are secondary cremations (“ustrinum”) found in funerary urns (Ortalli, 2017).

## 2. Materials and methods

### 2.1. Samples

We analysed 14 cremation deposits (12 tombs from the Via Emilia Est-Via Cesana necropolis and two tombs from the Via Emilia-

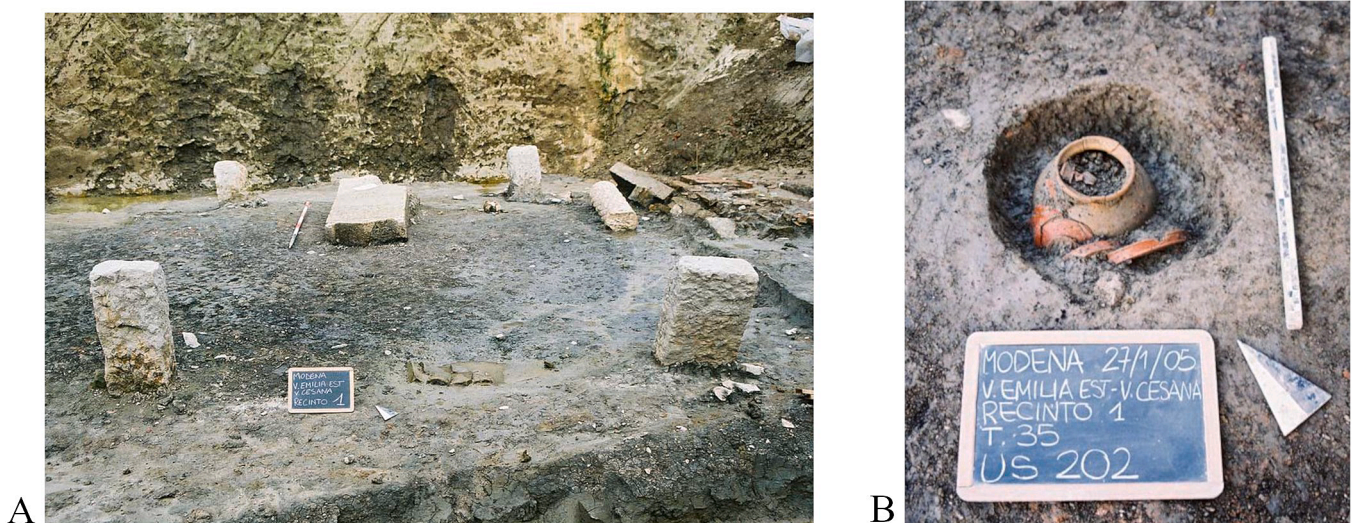


Fig. 1. Excavation of the necropolis of Via Emilia Est-Via Cesana. Funerary enclosure with a stele in the centre (A). Ceramic cinerary urn from Tomb 35 (B). From *mutinaromana.it*.

Tangenziale Pasternak necropolis). The two urban funerary contexts, excavated by Soprintendenza Archeologia, Belle Arti e Paesaggio per la Città Metropolitana di Bologna e le province di Modena, Reggio Emilia e Ferrara (Emilia-Romagna), are located close to the centre of the ancient Roman city of *Mutina*. We are aware that the number of individuals analysed in this study is small, limiting the interpretation of the results obtained. However, the main goal of the work is to set up a methodological backbone for future analyses of other Roman cemeteries in northern Italy.

An osteological analysis was conducted on each grave, beginning with the anatomical identification of each specific bone fragment. This was followed by the assessment of the minimum number of individuals (MNI) and the biological profile, estimating sex and age-at-death. The estimation of sex was based on the assessment of morphological traits typically characterised by sexually dimorphic traits (e.g., pelvis and skull; [Acsadi and Nemeskeri, 1974](#); [Buikstra and Ubelaker, 1994](#); [White and Folkens, 2012](#)). It was not possible to perform measurements on bones that exhibit sexual metric dimorphism, following [Cavazzuti et al. \(2019a\)](#), due to the lack of specific preserved skeletal portions. Age-at-death was estimated based on degenerative changes in specific skeletal areas, epiphyseal fusion stage, the fusion of epiphysis with diaphysis and the eruption and formation of teeth ([AlQahtani et al., 2010](#); [Brooks and Suchey, 1990](#); [Buikstra and Ubelaker, 1994](#)). Observations were also made regarding the presence of pathological conditions ([Ortner, 2003](#)) and the colour shade of the bone fragments, which can be attributed to the combustion temperature during the cremation process ([Walker et al., 2008](#)). Weight was not considered to estimate the minimum number of individuals and to assess their sex, as it is a debated and less reliable method due to its susceptibility to numerous variables ([Gonçalves et al., 2013](#)).

We selected a total number of 43 skeletal samples from the tombs, namely 14 fragments of diaphysis of long bones, 11 petrous bones, 12 fragments of ribs, and six tooth roots (the list of samples is in [Table 1](#)). These specific skeletal elements were chosen to assess different stages in the life-history of individuals (multi-tissue analysis). The petrous bone and dentin of tooth roots make it possible to trace the  $^{87}\text{Sr}/^{86}\text{Sr}$  value and the mobility pattern in the early years of life. The otic capsule of the petrous bone has an intrauterine formation and finishes its development by the age of two years, undergoing no further modification or remodelling ([Harvig et al., 2014](#); [Jørkov et al., 2009](#); [Veselka et al., 2021](#)). Root dentin forms and registers its signal during the period from mid to late childhood, depending on the tooth class considered ([AlQahtani et al., 2010](#)), due to minimal changes after its formation ([Nanci, 2003](#)). The only exception is the third molar, whose roots begin to form during adolescence ([AlQahtani et al., 2010](#)). The ribs, which constantly undergo remodelling (i.e., a physiological process necessary to maintain mineral homeostasis of the bones; [Katsimbri, 2017](#)), and the diaphysis of long bones (such as the femur) reflect adult strontium intake. Given that bone remodelling mainly occurs as a continuous process on bone surfaces, the ribs, with their thinner cortical bone, turn over more rapidly than long bones with their much thicker cortex. Other variables, such as the proximity to red bone marrow and location within the skeleton (axial or appendicular), are also relevant when considering turnover ([Parfitt, 2013](#)). However, as a general rule it can be ascertained that the ribs reflect the diet (or strontium intake) of the last few years of life of the individual ([Fahy et al., 2017](#); [Gosman et al., 2013](#); [Jørkov et al., 2009](#)), while the thick cortical bone of the femoral diaphysis reflects a much more substantial timespan ([ICRP, 1973](#); [Kerley, 1965](#)). For individuals who died as young adults or non-adults, it is important to factor in bone growth (bone modelling), whereby bone formation is more prevalent than resorption to facilitate the increase in size ([Kenkre and Bassett, 2018](#)). This means that strontium measurements for non-adults will reflect a shorter and more recent period in the individual's life.

The burials selected for the analysis were chosen based on the presence of the skeletal elements mentioned above. Particular attention

**Table 1**

List of samples selected from each tomb. Some tombs are only indicated with the number of their Stratigraphic Unit (US). The ID number is the code used to renominate each sample during isotope analysis. Regarding the petrous bone, it should be noted that the otic capsule was specifically sampled.

Site	Necropolis	ID	Tomb	US	Sample
Modena	Via Emilia Est – Via Cesana	FS001	53	30	Petrous bone
Modena	Via Emilia Est – Via Cesana	FS002	53	30	Tooth root
Modena	Via Emilia Est – Via Cesana	FS003	53	30	Rib
Modena	Via Emilia Est – Via Cesana	FS004	53	30	Diaphysis
Modena	Via Emilia Est – Via Cesana	FS005	36	210	Petrous bone
Modena	Via Emilia Est – Via Cesana	FS006	36	210	Diaphysis
Modena	Via Emilia Est – Via Cesana	FS007	56	317	Petrous bones
Modena	Via Emilia Est – Via Cesana	FS008	56	317	Rib
Modena	Via Emilia Est – Via Cesana	FS010	56	317	Diaphysis
Modena	Via Emilia Est – Via Cesana	FS011	58	324	Petrous bones
Modena	Via Emilia Est – Via Cesana	FS012	58	324	Tooth root
Modena	Via Emilia Est – Via Cesana	FS013	58	324	Rib
Modena	Via Emilia Est – Via Cesana	FS014	58	324	Diaphysis
Modena	Via Emilia Est – Via Cesana	FS016	52	194	Rib
Modena	Via Emilia Est – Via Cesana	FS017	52	194	Tooth root
Modena	Via Emilia Est – Via Cesana	FS018	52	194	Diaphysis
Modena	Via Emilia Est – Via Cesana	FS020	35	202	Rib
Modena	Via Emilia Est – Via Cesana	FS021	35	202	Diaphysis
Modena	Via Emilia Est – Via Cesana	FS022	46	284	Petrous bone
Modena	Via Emilia Est – Via Cesana	FS023	46	284	Tooth root
Modena	Via Emilia Est – Via Cesana	FS024	46	284	Rib
Modena	Via Emilia Est – Via Cesana	FS025	46	284	Diaphysis
Modena	Via Emilia Est – Via Cesana	FS026	8	109	Petrous bone
Modena	Via Emilia Est – Via Cesana	FS027	8	109	Rib
Modena	Via Emilia Est – Via Cesana	FS028	8	109	Diaphysis
Modena	Via Emilia Est – Via Cesana	FS029	1	71	Petrous bones
Modena	Via Emilia Est – Via Cesana	FS030	1	71	Rib
Modena	Via Emilia Est – Via Cesana	FS031	1	71	Diaphysis
Modena	Via Emilia Est – Via Cesana	FS032	/	103	Petrous bone
Modena	Via Emilia Est – Via Cesana	FS033	/	103	Diaphysis
Modena	Via Emilia Est – Via Cesana	FS034	/	78	Rib
Modena	Via Emilia Est – Via Cesana	FS036	/	78	Diaphysis
Modena	Via Emilia – Tangenziale Pasternak	FS037	14	243	Diaphysis
Modena	Via Emilia – Tangenziale Pasternak	FS038	14	243	Rib
Modena	Via Emilia – Tangenziale Pasternak	FS039	14	243	Tooth roots
Modena	Via Emilia – Tangenziale Pasternak	FS040	14	243	Petrous bone
Modena	Via Emilia – Tangenziale Pasternak	FS041	10	203	Diaphysis
Modena	Via Emilia – Tangenziale Pasternak	FS042	10	203	Rib
Modena	Via Emilia – Tangenziale Pasternak	FS043	10	203	Tooth root
Modena	Via Emilia – Tangenziale Pasternak	FS044	10	203	Petrous bone
Modena	Via Emilia Est – Via Cesana	FS045	4	/	Petrous bones
Modena	Via Emilia Est – Via Cesana	FS046	4	/	Diaphysis
Modena	Via Emilia Est – Via Cesana	FS048	4	/	Rib

was given to burials with the presence of petrous bones, as these are the elements that reflect the strontium intake of the early life stages of the individual. In addition, to avoid problems of contamination by diagenesis, only completely calcined bone fragments (i.e., white colouring) were selected ([Snoeck et al., 2015](#); [Walker et al., 2008](#)).

## 2.2. Strontium isotope analysis

For the  $^{87}\text{Sr}/^{86}\text{Sr}$  analysis we followed the procedure described in Snoeck et al. (2015). The analysis was performed at the Research Unit: Archaeology, Environmental Changes & Geo-Chemistry (AMGC) at the Vrije Universiteit Brussel (VUB), Belgium.

Before starting with the strontium analysis, bone samples were mechanically and chemically pre-treated. Sediment and any visible surface contaminants were first removed from each fragment (with a minimum weight of 200 mg) with a diamond burr mounted on a hand-held Dremel, to remove the outer cortical surface potentially affected by diagenesis. This step is particularly important to establish the actual colour of the bone (since sometimes sediment or minerals, such as manganese, can alter its true shade) and to assess the temperature phase to which it was exposed during cremation. For petrous bones, we followed the procedure described in Veselka et al. (2021). Each petrous bone was cut transversely in half through the internal acoustic meatus using a rotating wheel with diamond cutting edge mounted on a Dremel multitool. Then, sediment and surface contaminants were removed from both the outer and inner surfaces of the two cut portions of each petrous bone. We then proceeded to chemically pre-treat each sample, following McMillan et al. (2019) and Snoeck et al. (2015), by rinsing three times with MilliQ water in the ultrasonic bath for ten minutes. Each sample was then treated with 10 mL of 1 M acetic acid ( $\text{CH}_3\text{COOH}$ ; acetic acid is used to remove secondary carbonates, usually accumulated during diagenetic processes) for ten minutes in the ultrasonic bath, and then rinsed a further three times with MilliQ water in the ultrasonic bath for ten minutes. After that, the samples were placed in the oven (with a temperature of approximately  $50^\circ\text{C}$ ) until they were completely dry. Mechanical and chemical pre-treatment made it possible to further select the samples chosen for analysis, excluding those that only appeared completely calcined, but were in fact at a less advanced stage of combustion. This is frequently the case with petrous bones, which, while appearing calcined on the outside, may have remained more protected on the inside, thus only being charred. Of the 43 starting samples, 33 were found to be truly suitable and selected for isotope analysis. Long bone diaphysis and rib fragments, once dry after pre-treatment, were reduced to powder using a marble mortar and pestle. Tooth roots were sampled by abrading the surface with a diamond-tipped burr mounted on a hand-held Dremel. With the same diamond-tipped burr, only the surfaces of the otic capsule (cochlea, vestibule and semicircular canals), characterised by almost no turnover after the age of c. 2, were sampled (Veselka et al., 2021). The powder obtained from the samples was then weighed ( $\sim 15$  mg) and transferred into Teflon beakers.

Each sample was reacted with 1 mL of 14 M nitric acid ( $\text{HNO}_3$ ) until complete dissolution of the powder. Each beaker was placed on the hot plate ( $90^\circ\text{C}$ ) for 2 h. Once the sample was completely dissolved, each beaker was left without lid on the hot plate ( $100^\circ\text{--}110^\circ\text{C}$ ) overnight to dry the sample and evaporate the acid. Next, 2.5 mL of 7 M  $\text{HNO}_3$  was added to each beaker, which was then placed in the ultrasonic bath for 20 min. Strontium was extracted using column chemistry with ion exchange Sr-spec resin (Triskem<sup>TM</sup>). The columns were rinsed with 1 mL of 2 M  $\text{HNO}_3$ , then filled with approximately 1 mL of resin and rinsed again with 1 mL of 2 M  $\text{HNO}_3$ . Then, 1 mL of 7 M  $\text{HNO}_3$  was added into the columns two times. After that, 0.5 mL of each sample was loaded into the corresponding column. This step was repeated three additional times. Then, to rinse the columns, 1 mL of 7 M  $\text{HNO}_3$  and the remaining sample were added to each column. To rinse the resin, 1 mL of 7 M  $\text{HNO}_3$  was added four times. Finally, for the elution of Sr, 1 mL of 0.05 M  $\text{HNO}_3$  was added six times, the sample evaporated to dryness, then redissolved in 1.5 mL 0.05 M  $\text{HNO}_3$  for analysis.

The  $^{87}\text{Sr}/^{86}\text{Sr}$  ratio was determined with a Nu Plasma 3 MC-ICP-MS (PD017 from Nu Instruments, Wrexham, UK) at the Vrije Universiteit Brussel. During each analysis, structured in 2 blocks of 30 cycles (for a total of 60 ratio measurements), the following  $m/z$  were acquired:  $^{83}\text{Kr}$ ,

$^{84}\text{Sr}$ ,  $^{85}\text{Rb}$ ,  $^{86}\text{Sr}$ ,  $^{87}\text{Sr}$  and  $^{88}\text{Sr}$ . Rb and Kr interference correction followed routine protocols (Gerritzen et al., 2024; Snoeck et al., 2015). The  $^{87}\text{Sr}/^{86}\text{Sr}$  ratio was normalised using an exponential law to  $^{86}\text{Sr}/^{88}\text{Sr} = 0.1194$ . Repeated measurements of the NBS987 standard produced  $^{87}\text{Sr}/^{86}\text{Sr} = 0.710243 \pm 0.000031$  (2SD for  $>140$  analyses), which is consistent with the mean value of  $0.710252 \pm 0.000013$  (2SD for 88 analyses) obtained by Thermal Ionization Mass Spectrometry (TIMS) instrumentation (Weis et al., 2006). All the measurements were normalised to the recommended value of  $^{87}\text{Sr}/^{86}\text{Sr} = 0.710248$  (Weis et al., 2006) using a standard bracketing method. Procedural blanks were considered negligible (total Sr (V) of max 0.02 versus 10 V for analyses; i.e.  $\approx 0.2\%$ ).

## 2.3. Bioavailable strontium isotope range

The territory of the city of Modena falls within the Po Valley and is less than ten kilometres from the slopes of the Apennines, linking its position to the slope of the mountain range and the depression of the floodplain. The surface geolithology is mainly characterised by alluvial deposits, settled at the end of the Pleistocene and during the Holocene. Beneath the exposed alluvial deposits lie older marine sediments from the Pliocene and Pleistocene epochs (Bally et al., 1985).

The “local human range” for this study was determined using the Tukey’s interquartile range method (or Tukey’s fences [ $Q1 - k(Q3 - Q1)$ ,  $Q3 + k(Q3 - Q1)$ ], with  $k = 1.5$ ; Lightfoot and O’Connell, 2016) on all human data. To check for the consistency of this range with the natural variability in the Modena area, we used comparison literature data (see Fig. 2 and Lugli et al., 2022 for an overview) and the Italian Sr isoscape (Universal Kriging model; Lugli et al., 2022). From this model, we

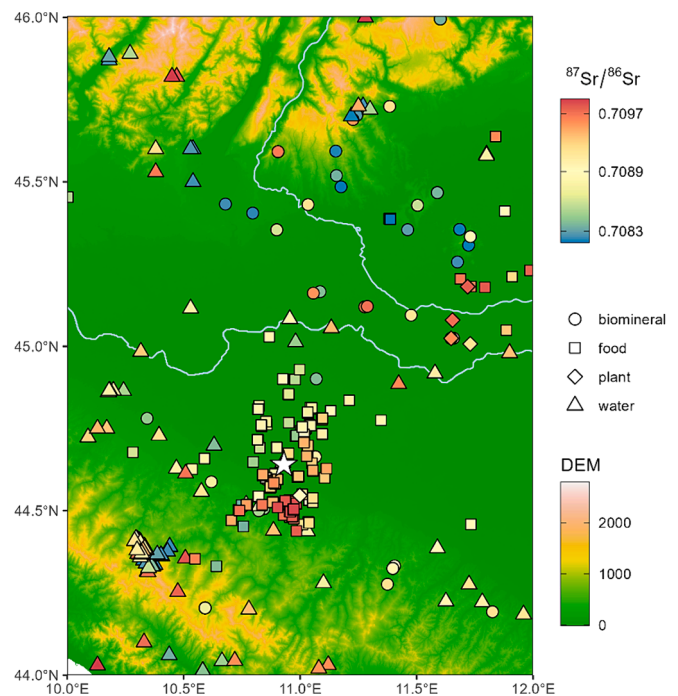


**Fig. 2.** Compilation of bioavailable Sr isotope data from literature, including biominerals (snails, dentin and bioapatite), food samples (apple and wine branches), plants, soil leachates and waters (Aviani, 2013; Boschetti et al., 2005; Boschetti et al., 2011; Cavazzuti et al., 2019b; Conti et al., 2000; Deiana et al., 2018; Durante et al., 2015; Durante et al., 2018; Francisci et al., 2020; Lugli et al., 2018; Marchina et al., 2018), coloured according to their Sr isotope ratio;  $^{87}\text{Sr}/^{86}\text{Sr}$  values are represented with a quantile ( $q_{0.1}$ , median,  $q_{0.9}$ ) scale. We are aware that food samples may be contaminated by modern fertilisers and other anthropogenic sources, but they have been retained in the figure because they are consistent with other biogenic samples. Data are plotted over a SRTM Digital Elevation Model (DEM) in m from CGIAR-CSI. The white star is Modena.

extracted pixels at different buffer radii around the site, yielding  $^{87}\text{Sr}/^{86}\text{Sr}$  quartiles (Q1-Q3) of 0.70884–0.70901, 0.70878–0.70907, 0.70872–0.70908 and 0.70870–0.70906, for 5, 10, 15 and 20 km respectively.

### 2.4. Mobility and provenance analyses

To test the geographical provenance of non-local individuals we used the *assignR* package (Ma et al., 2020) through R v. 4.1.2 (R Development Core Team, 2021). Ma et al.'s method employs a Bayesian protocol, assuming equal likelihood across grid cells as the prior probability for an individual's origin. Using isotope ratios, it calculates the posterior probability of sample origin for each grid cell, generating a raster object with probability density surfaces for each sample and their probable provenance. The bioavailable Universal Kriging map of Lugli et al. (2022) was used as a reference raster, associated with a variable prediction error (standard deviation) (see Esposito et al., 2023 and <https://www.geochem.unimore.it/sr-isoscape-of-italy/>). It should be noted that the best approach would involve the use of several different isotopes to make inferences on geographical origin; in this work, the limitations imposed by cremated remains did not allow us to use other isotopes besides  $^{87}\text{Sr}/^{86}\text{Sr}$  (without risking contamination by external factors; Salesse et al., 2021; Stamataki et al., 2021).

## 3. Results

### 3.1. Osteological study of cremations from the necropoleis of Mutina

The osteological study of the cremated remains from the 14 tombs selected for this research (12 tombs from the Via Emilia Est-Via Cesana necropolis and two tombs from the Via Emilia-Tangenziale Pasternak necropolis) made it possible to identify a minimum number of 14 individuals, as no details suggesting the presence of more than one individual were noted (e.g., the repetition of the same skeletal elements or inconsistencies regarding the biological profile of the individual in each grave). In general, the osteological material was very fragmented, with fragments rarely exceeding 5 cm in length. The most frequently encountered types of heat-related fractures were conchoid, longitudinal and transverse. Except for rare cases, the bone fragments analysed were very light coloured (light grey-white or completely white), which can be attributed to an advanced combustion temperature (above 800–900 °C). Out of 14 cremations, it was possible to estimate sex and/or age-at-death for seven individuals (Table 2): two young adults (Tombs 14, 58) and five adults (Tombs 4, 10, 36, 52, 53) of which two are males (Tombs 10 and 53). Information about the biological profile of the individual of Tomb 10 was taken from Higgins et al. (2020). The other cremations had no preserved diagnostic elements useful for the evaluation of the biological profile. No pathological conditions were recognised. Along with

**Table 2**

Tombs from Roman necropoleis of Mutina and the results from the osteological studies of MNI, age-at-death and sex.

Tombs	Necropolis	MNI	Age class	Sex
53	Via Emilia Est – Via Cesana	1	Adult	Male
36	Via Emilia Est – Via Cesana	1	Adult	/
56	Via Emilia Est – Via Cesana	1	/	/
58	Via Emilia Est – Via Cesana	1	Young adult	/
52	Via Emilia Est – Via Cesana	1	Adult	/
35	Via Emilia Est – Via Cesana	1	/	/
46	Via Emilia Est – Via Cesana	1	/	/
8	Via Emilia Est – Via Cesana	1	/	/
1	Via Emilia Est – Via Cesana	1	/	/
US 103	Via Emilia Est – Via Cesana	1	/	/
US 78	Via Emilia Est – Via Cesana	1	/	/
14	Via Emilia – Tangenziale Pasternak	1	Young adult	/
10	Via Emilia – Tangenziale Pasternak	1	Adult	Male
4	Via Emilia Est – Via Cesana	1	Adult	/

human bones, in some cases, animal bones, charcoal, glass and pottery fragments were also found, and these were almost certainly grave goods. Particularly notable are the engraved fragments of funerary beds made using animal bones.

### 3.2. $^{87}\text{Sr}/^{86}\text{Sr}$ results of cremated human remains

The values of  $^{87}\text{Sr}/^{86}\text{Sr}$  obtained from the 33 samples from Modena are provided in Table 3. For each sample, the strontium value is reported with a 2 SE error (internal standard error of each analysed sample). The  $^{87}\text{Sr}/^{86}\text{Sr}$  values range between 0.70816 and 0.71069. The mean value is 0.70901, the median value is 0.70890 and the Tukey interval is between 0.70851 and 0.70934. Our estimate of Tukey interval includes multiple samples from the same grave (and possibly from the same individual). For this reason, we are aware that the estimate may be biased, but, at the same time, the  $^{87}\text{Sr}/^{86}\text{Sr}$  values of the Tukey fences (Tukey's interquartile range method) are consistent with the biogenic values around the Modena area, as observed in Lugli et al. (2022) and in the Italian isoscape (Fig. 3).

Nine samples fall outside the local bioavailable strontium range (Fig. 4; Table 3), suggesting a different mobility pattern and origin of some individuals buried in the investigated necropoleis. The samples are two rib fragments (FS020, FS016), two petrous bones (FS011, FS044), four diaphysis fragments (FS028, FS018, FS031, FS021) and one tooth root (FS023). The samples derive from seven tombs, as some of them belong to the same grave: Tb 1 (FS031), Tb 8 (FS028), Tb 10 (FS044), Tb 35 (FS020, FS021), Tb 46 (FS023), Tb 52 (FS016, FS018) and Tb 58 (FS011), and have  $^{87}\text{Sr}/^{86}\text{Sr}$  values between 0.70816 and 0.71069 (mean = 0.70901±0.00059). All the tombs, except for grave 10 which comes from Via Emilia-Tangenziale Pasternak, come from Via Emilia Est-Via Cesana. Of these individuals, it was only possible to estimate the age-at-death and/or sex in three cases: an adult male (Tomb 10; for more

**Table 3**

Strontium isotope results for each sample. In addition to the  $^{87}\text{Sr}/^{86}\text{Sr}$  value, the in-run error (2 SE) is also indicated.

ID	Grave	Sample	$^{87}\text{Sr}/^{86}\text{Sr}$	2SE
FS002	53	Tooth root	0.709080	0.000010
FS004	53	Diaphysis	0.708838	0.000009
FS006	36	Diaphysis	0.709265	0.000009
FS007	56	Petrous bone	0.708842	0.000008
FS008	56	Rib	0.708844	0.000009
FS011	58	Petrous bone	0.708302	0.000008
FS012	58	Tooth root	0.708851	0.000008
FS013	58	Rib	0.708883	0.000009
FS014	58	Diaphysis	0.708797	0.000008
FS016	52	Rib	0.708400	0.000008
FS017	52	Tooth root	0.708709	0.000009
FS018	52	Diaphysis	0.708471	0.000009
FS020	35	Rib	0.708161	0.000007
FS021	35	Diaphysis	0.710696	0.000008
FS023	46	Tooth root	0.709980	0.000008
FS024	46	Rib	0.708968	0.000010
FS027	8	Rib	0.708809	0.000007
FS028	8	Diaphysis	0.708465	0.000009
FS029	1	Petrous bone	0.709224	0.000008
FS030	1	Rib	0.708883	0.000010
FS031	1	Diaphysis	0.709645	0.000008
FS033	US 103	Diaphysis	0.708903	0.000009
FS034	US 78	Rib	0.708852	0.000009
FS036	US 78	Diaphysis	0.708823	0.000008
FS037	14	Diaphysis	0.709011	0.000010
FS038	14	Rib	0.708937	0.000010
FS039	14	Tooth root	0.709027	0.000009
FS040	14	Petrous bone	0.708967	0.000010
FS041	10	Diaphysis	0.709028	0.000009
FS042	10	Rib	0.708993	0.000008
FS043	10	Tooth root	0.708904	0.000007
FS044	10	Petrous bone	0.710628	0.000007
FS045	4	Petrous bone	0.709064	0.000009

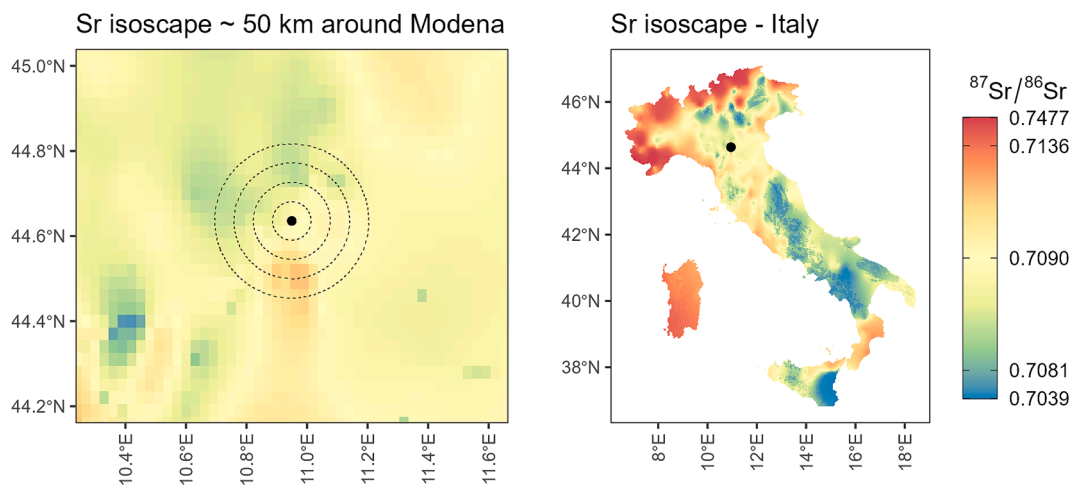


**Fig. 3.** Bioavailable Sr isoscape around the city of Modena (~50 km), identified by the black dot. The buffer radii correspond to 5, 10, 15 and 20 km around Modena (left panel). Italian Sr isoscape (right panel). Data are represented through a quantile colour scale ( $q_{0.1}$ , median,  $q_{0.9}$ ); the maximum and the minimum values are also reported.

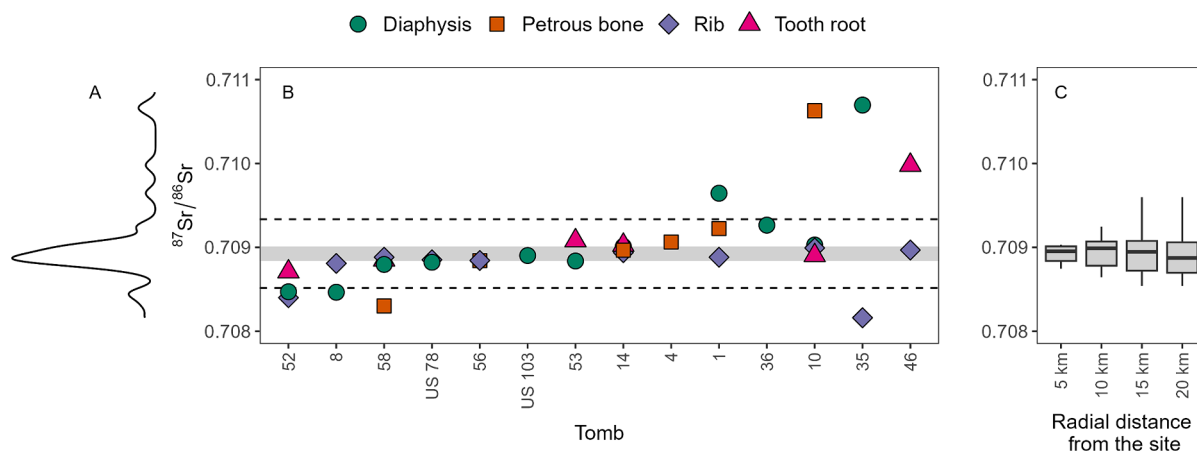


**Fig. 4.** A) Kernel density estimate of the Sr sample distribution. B) Sr isotopes of samples grouped by tomb and ordered by ascending average Sr isotope ratio; different body parts analysed are represented with different colours and shapes: diaphysis as green circle, petrous bone as orange square, rib as purple diamond and tooth root as pink triangle; the distribution of the samples suggests the presence of probable multiple burials (very likely for Tomb 35, and conceivable for Tombs 52, 8, 58, 1, 10, 46) due to inconsistencies in terms of individuals' life-histories. Dashed lines represent the Tukey fences; the grey area is the local  $^{87}\text{Sr}/^{86}\text{Sr}$  range 5 km around Modena extracted from the isoscape. C) Box-plots representing Sr isotope ratios extracted from the Italian isoscape at different radial distances from the site. (For interpretation of the references to colour in this figure legend, the reader is referred to the web version of this article.)

details see Higgins et al., 2020), an adult (Tomb 52) and a young adult (Tomb 58), whose sex could not be estimated.

#### 4. Discussion

Fig. 4 shows the dispersion in  $^{87}\text{Sr}/^{86}\text{Sr}$  of the samples, grouped for each tomb and compared with the expected local bioavailable  $^{87}\text{Sr}/^{86}\text{Sr}$  of the city of Modena, at radial distances of 5, 10, 15 and 20 km from the site (Lugli et al., 2022). The results suggest that some of the individuals analysed spent part of their lives in areas other than *Mutina*, long enough to alter the isotopic signal of their skeletal tissues. In fact, their isotopic ratios do not fall within the bioavailable strontium (BASr) ratio of the Modena surroundings. The presence of non-local  $^{87}\text{Sr}/^{86}\text{Sr}$  values of some petrous bones and tooth roots suggest that some individuals were born in other localities and then moved to *Mutina*, where they were buried. On the other hand, the non-local signal detected in rib and diaphysis fragments is related to people who moved to *Mutina* only in the last years of their lives, explaining why, despite bone remodelling, the bone tissue does not reflect the local signal but that of the place of origin. It is interesting to note how Tomb 52 contains human remains of

an individual who may have been born in *Mutina* (considering the local signal obtained from the dentin of the tooth root) and then moved or consumed food in a place with a slightly less radiogenic Sr isotope ratio. The individual returned to *Mutina*, where they died (or returned after death), without their ribs and diaphysis had the time to fully reflect the local Sr range. Considering that the turnover rate of long bones is less rapid than that of ribs (Jørkov et al., 2009), it is likely that Tomb 8 contains the human remains of a single individual, who spent part of their life in a place other than *Mutina* (considering the difference between diaphysis and rib), and then moved there during their last years of life. Tomb 58 could contain the remains of one individual who was born outside *Mutina*, considering the  $^{87}\text{Sr}/^{86}\text{Sr}$  values of the petrous bone, and then moved in early childhood, as indicated by the local  $^{87}\text{Sr}/^{86}\text{Sr}$  values registered by the tooth root. Although it is more plausible that the isotopic signal reflects the intake of  $^{87}\text{Sr}/^{86}\text{Sr}$  within the first two years of the individual's life after birth (considering the rapid remodelling of this bone), it is also useful to consider that the otic capsule begins its formation at 18/19 weeks in utero. Due to the stress that breastfeeding causes to the maternal skeleton, releasing calcium (and by extension Sr) reserves (Kovacs, 2016), the isotopic signal may also reflect the mother's

mobility. For Tomb 1, the difference in strontium values recorded by the rib and diaphysis fragments can be explained by the different turnover rates in the two different bones: in the meantime the diaphysis has shifted towards the *Mutina* signature, the rib fragment had completely overprinted. The data suggest that this could be an individual who was born and died in *Mutina*, but spent most of their life elsewhere. Tomb 10 likely contains the remains of a single individual who moved to *Mutina* during their early childhood, considering the high radiogenic strontium values expressed by the petrous bone and the isotopic ratio of the other bones which fit within the local BASr of Modena. Again, although less plausible, we should consider that the otic capsule may also reflect the isotopic signal of the mobility of the mother. Tomb 35 is likely to contain more than one individual, as the rib and the diaphysis fragments are very different, representing the less and the most radiogenic value of all the samples. However, if the difference in turnover rate between long bones and ribs is considered, it is possible to assume that the remains belong to a single individual who moved from one area to another. Tomb 46 likely contains one individual, who was born in areas outside *Mutina* and then moved and died there (considering the different values of the dentin of the tooth root and the rib fragment). The presence of more than one individual is very likely for Tomb 35 and conceivable for many of these tombs, although the low difference between the  $^{87}\text{Sr}/^{86}\text{Sr}$  values, also due to the difference in bone turnover, must be taken into account. The presence of multiple individuals was not detected through the classic anthropological study carried out, since all the preserved human remains correspond to one individual for each grave. All the other tombs likely contain one local individual. Unfortunately, due to a lack of suitable material for the isotope analysis (i.e., the bones were not present, the bones were present but were not properly calcined), it is not possible to assess the mobility pattern for Tombs 4 and 36, and for US 78 and 103.

We evaluated the provenance probability of these outliers, and Fig. 5 shows the areas (in yellow) with the top 5 % probability of origin of the nine outliers.

Yet, the isotopic signal recorded in long bones and ribs, in comparison to petrous bones and tooth roots, is the result of strontium intake that occurred over an extended period of time. Hence, the observed  $^{87}\text{Sr}/^{86}\text{Sr}$  signals could result from a single (relatively) homogeneous Sr source over time, or from the mix of different end-members linked to geologically different locations. Overall, the impact of this effect differs between ribs and long bones due to their different turnover/remodelling rates (Kenkre and Bassett, 2018). Ribs, in fact, have very thin cortical bone and a high surface to volume ratio, leading to a high rate of remodelling and thus reflecting the isotopic signal of a shorter and more recent period in an individual's life (ICRP, 1973). However, it should also be specified that with increasing age, the rate of bone remodelling tends to decrease (especially in women), as the rate of resorption is higher than the rate of new tissue formation (Katsimbri, 2017; Martin and Seeman, 2008; Parfitt, 2013). Unfortunately, it was only possible to estimate an age class for seven of the 14 tombs examined, five of which contained human remains belonging to adult individuals (Table 2). It is likely, therefore, that their remodelling rate is lower than that of younger individuals, making them less affected by isotopic variations due to displacement or consumption of food from different geological substrates.

Using the isotope-based method for geographical assignment described in Ma et al. (2020), we investigated the most likely origin of each non-local individual across the Italian landscape. We acknowledge that, specifically for long bone and rib samples, the abovementioned bone remodelling hinders a proper interpretation of provenance maps, thus read with caution (Fig. 5).

The outliers with  $^{87}\text{Sr}/^{86}\text{Sr}$  values of 0.71069 and 0.71062 (FS021 and FS044, respectively) show similar areas with the highest probability of origin, which are mainly located in northern Italy and probably in (Pre)Alpine areas. The outliers with  $^{87}\text{Sr}/^{86}\text{Sr}$  values of 0.70998 and 0.70964 (FS023 and FS031, respectively) show possible isotopic

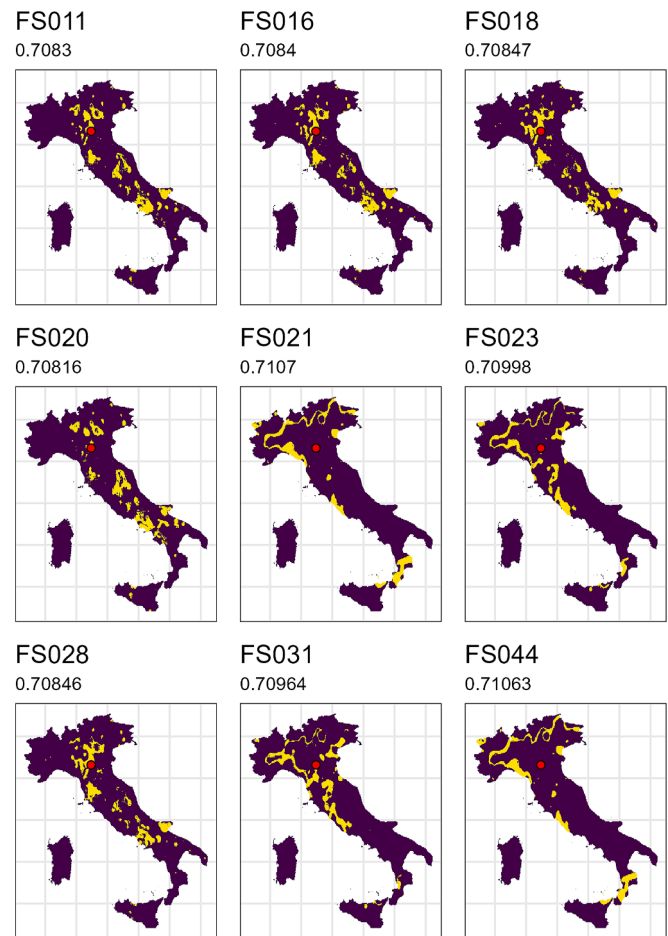


Fig. 5. The yellow areas represent the top 5 % probability of origin of  $n = 9$  outliers, based on the Bayesian workflow of Ma et al. (2020). The red dot is the city of Modena. (For interpretation of the references to colour in this figure legend, the reader is referred to the web version of this article.)

compatible areas located in northern/central Italy, such as Veneto and Tuscany, if we look at closest regions (Lugli et al., 2022). Outliers with  $^{87}\text{Sr}/^{86}\text{Sr}$  values between 0.70816 and 0.70847 (FS011, FS016, FS018, FS020 and FS028) show similar areas with the highest probability of origin, and they could have originated not far from the city of Modena and the Po Valley in general (Lugli et al., 2022). Considering the relatively high radiogenic values of some of the samples, which are only partially compatible with the ratios found in alluvial deposits of the Po Valley, it is possible that some of the outlier individuals, especially ones with the most radiogenic values, came from the (Pre)Alpine areas and, at different times in their lives, moved to *Mutina*.

The  $^{87}\text{Sr}/^{86}\text{Sr}$  isotope baseline in the Po Valley is intriguing. In the northern parts, the geolithology of the environment is varied and differentiated, resulting in a broad range of strontium values, while the southern parts of the Po River feature fewer geolithological units and a narrower  $^{87}\text{Sr}/^{86}\text{Sr}$  isotope baseline (Cavazzuti et al., 2019b). Furthermore, it should be noted that high radiogenic  $^{87}\text{Sr}/^{86}\text{Sr}$  values (0.7098–0.7123) have also been recorded in hilly areas close to Modena (e.g., Castelvetto, Vignola, Savignano sul Panaro), although these values come from modern and anthropogenic vine branches and soil samples (Durante et al., 2018).

For the first time, it is possible to combine information on mobility and provenance from isotopes analysis with the cultural information provided by the grave goods in the Roman necropoleis of *Mutina*. The hypothesis of a provenance from the Alpine and (Pre)Alpine areas for the more radiogenic outliers is further supported by the grave goods

found in Tomb 15 (not sampled for isotopic analysis; see section 2.1) in the necropolis of Via Emilia Est-Via Cesana. Tomb 15, excavated in 2004–2005 and contemporaneous with the graves analysed in this study, contains the human remains of two individuals from a secondary cremation: an infant (4–6 years old) and an adult; the latter is defined as a female by the anthropologists who studied the burial based on the grave goods (Ortalli, 2017). However, it is necessary to reiterate the difficulty in estimating the sex of cremated individuals and to emphasise that the grave goods are not always a reliable indicator of biological sex.

The grave goods include “standard” objects, commonly found in the necropoleis of Modena during the Roman Empire (e.g., oil lamps, ceramic cups, ornamental objects; Ortalli, 2011), with a few exceptions. The soapstone urn and a glass balsam jar (with a peculiar shape called “a colombina”) suggest an origin other than *Mutina* (Fig. 6). For both of them, the most likely area of production and dissemination is the western (Pre)Alpine area (Dr. Silvia Pellegrini, personal communication; Ansaloni and Sala, 2017; Corti, 2017; furthermore, see Poletti Ecclesia and Tassinari, 2016 for a direct comparison with soapstone urns and Brecciaroli Taborelli, 2011 for a direct comparison with glass balsam jars found in the (Pre)Alpine area of present-day Lombardy and Piedmont).

## 5. Conclusions

The purpose of this study was to investigate the human mobility of individuals buried in the Roman city of *Mutina*. This investigation is based on the assumption that cremated human remains are a reliable substrate for the preservation of strontium isotopes. The study was conducted on two necropoleis that exclusively featured cremation as a burial ritual: Via Emilia Est-Via Cesana and Via Emilia-Tangenziale Pasternak. The results suggest that some individuals had origins or spent part of their lives in areas other than *Mutina*, where they were buried. Considering the more radiogenic strontium values of some of the samples, which were incompatible with the ratios found in the alluvial deposits of the Po Valley, it is likely that some of the individuals came from (Pre)Alpine areas. This finding is further supported by the presence of grave goods in Tomb 15 (Via Emilia Est-Via Cesana necropolis), which include non-local objects (in terms of manufacture and raw materials), which were instead widespread in the western (Pre)Alpine area of present-day Lombardy and Piedmont. The results of this study show that strontium isotope analysis supported the estimations of traditional osteological studies, such as the minimum number of individuals, and allowed the investigation of human mobility from cremated remains. Future research aims to improve this study by selecting other contemporaneous necropoleis in *Mutina* for strontium isotope analysis, as well as to proceed with the analysis using other isotopes systematics (e.g., neodymium) to assess the range of supply and dissemination of raw materials for grave goods that appear to be of non-local provenance.

## CRediT authorship contribution statement

**Francesca Seghi:** Writing – review & editing, Writing – original draft, Visualization, Methodology, Investigation, Funding acquisition, Formal analysis, Data curation, Conceptualization. **Federico Lugli:** Writing – review & editing, Writing – original draft, Visualization, Validation, Methodology, Formal analysis, Data curation, Conceptualization. **Hannah F. James:** Writing – review & editing, Validation, Methodology, Formal analysis. **Tessi Löffelmann:** Writing – review & editing, Validation, Methodology, Formal analysis. **Elena Armaroli:** Writing – review & editing. **Antonino Vazzana:** Writing – review & editing. **Anna Cipriani:** Writing – review & editing, Resources. **Christophe Snoeck:** Writing – review & editing, Validation, Supervision, Resources, Methodology, Funding acquisition, Formal analysis, Conceptualization. **Stefano Benazzi:** Writing – review & editing, Supervision, Resources, Funding acquisition.

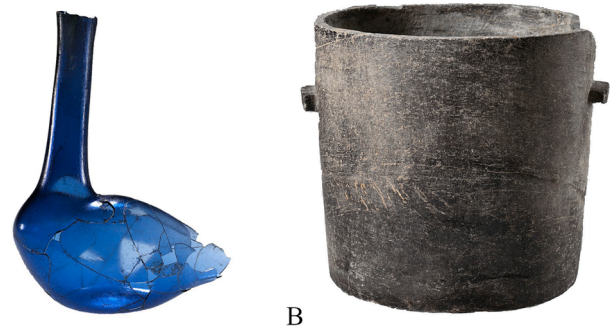


Fig. 6. The glass balsam jar (A) and soapstone urn (B) found in Tomb 15 of the necropolis of Via Emilia Est-Via Cesana. Image modified after Corti, 2017.

## Declaration of Competing Interest

The authors declare that they have no known competing financial interests or personal relationships that could have appeared to influence the work reported in this paper.

## Data availability

Data will be made available on request.

## Acknowledgments

This research project was promoted by Soprintendenza Archeologia, Belle Arti e Paesaggio per la Città Metropolitana di Bologna e le province di Modena, Reggio Emilia e Ferrara. Heartfelt thanks go to Cinzia Cavallari, who passed away prematurely in 2022, for initiating the project on the Funeral Rituals of *Mutina*. We thank Museo Civico di Modena, particularly Silvia Pellegrini, for permission to study and access the materials, and for support and all archaeological information. This publication is based upon work from COST Action INEAL, CA19141, supported by COST (European Cooperation in Science and Technology). This work was supported by the ERC Starting Grant LUMIERE (Landscape Use and Mobility In Europe-Bridging the gap between cremation and inhumation, grant number 948913), funded by European Union's Horizon 2020 Research and Innovation programme. FL is supported by the Marie Skłodowska-Curie IF actions AROUSE (Assessing the Impact of Climate Fluctuations on Hibernation Phenology using Novel Dental Biomarkers, grant number 101104566), funded by European Union's Horizon Research and Innovation programme.

## References

- Acsadi, G.I., Nemeskeri, J., 1974. History of Human Life Span and Mortality. *Curr. Anthropol.* 15, 495–507.
- AlQahtani, S.J., Hector, M.P., Liversidge, H.M., 2010. Brief Communication: The London Atlas of Human Tooth Development and Eruption. *Am. J. Phys. Anthropol.* 42, 481–490.
- Ansaloni, I., Sala, L., 2017. *Mutina* lo spazio funerario. Tomba 15. In: Malnati, L., Pellegrini, S., Piccinini, F. (Eds.), *Mutina* splendissima. La città Romana e la sua eredità. Modena.
- Aviani, U., 2013. Applicazione della sistematica isotopica dello Sr alla tracciabilità e alla qualificazione di prodotti vitivinicoli: studio sul Prosecco veneto. PhD thesis. University of Trieste.
- Bally, A.W., Catalano, R., Oldow, J., 1985. Elementi Di Tettonica Regionale, Evoluzione Dei Bacini Sedimentari e Delle Catene Montuose. Pitagora Editrice Bologna.
- Bentley, R.A., 2006. Strontium isotopes from the earth to the archaeological skeleton: a review. *J. Archaeol. Method Theory* 13, 135–187.
- Boschetti, T., Venturini, G., Toscani, L., Barbieri, M., Mucchino, C., 2005. The Bagni di Lucca thermal waters (Tuscany, Italy): an example of Ca-SO<sub>4</sub> waters with high Na/Cl and low Ca/SO<sub>4</sub> ratios. *J. Hydrol.* 307 (1–4), 270–293.
- Boschetti, T., Toscani, L., Shouakar-Stash, O., Iacumin, P., Venturini, G., Mucchino, C., Frappe, S.K., 2011. Salt waters of the Northern Apennine Foredeep Basin (Italy): origin and evolution. *Aquat. Geochim.* 17 (1), 71–108.
- Brecciaroli Taborelli, L., 2011. Vasellame e contenitori in vetro. In: *Oro pane e scrittura. Memorie di una comunità inter Vercellas et Eporediam*. Roma.



- Brooks, S., Suchey, J.M., 1990. Skeletal age determination based on the os pubis: A comparison of the Acsadi-Nemeskeri and Suchey-Brooks methods. *Hum. Evol.* 5, 227–238.
- Buikstra, J.E., Ubelaker, D.H., 1994. Standards for Data Collection from Human Skeletal Remains: Proceedings of a Seminar at the Field Museum of Natural History (Arkansas Archeological Report Research Series). In: Jonatha, H., Buikstra, J.E., Ubelaker, D. H., Aftandilian, D. (Eds.), Proceedings of a Seminar at the Field Museum of Natural History. Arkansas Archeological Survey.
- Cavazzuti, C., Bresadola, B., d'Innocenzo, C., Interlando, S., Sperduti, A., 2019a. Towards a new osteometric method for sexing ancient cremated human remains. Analysis of Late Bronze Age and Iron Age samples from Italy with gendered grave goods. *PLoS One* 14, 1–21.
- Cavazzuti, C., Skeates, R., Millard, A.R., Nowell, G., Peterkin, J., Brea, M.B., Cardarelli, A., Salzani, L., 2019b. Flows of people in villages and large centres in Bronze Age Italy through strontium and oxygen isotopes. *PLoS One* 14 (1), e0209693.
- Conti, A., Sacchi, E., Chiarle, M., Martinelli, G., Zuppi, G.M., 2000. Geochemistry of the formation waters in the Po plain (Northern Italy): an overview. *Appl. Geochem.* 15 (1), 51–65.
- Corti, C., 2017. *Mutina* lo spazio funerario. Tomba 15. In: Malnati, L., Pellegrini, S., Piccinini, F. (Eds.), *Mutina* splendidissima. La città Romana e la sua eredità. Modena.
- Deiana, M., Cervi, F., Pennisi, M., Mussi, M., Bertrand, C., Tazioli, A., Corsini, A., Ronchetti, F., 2018. Chemical and isotopic investigations ( $\delta^{18}\text{O}$ ,  $\delta^2\text{H}$ ,  $^3\text{H}$ ,  $^{87}\text{Sr}/^{86}\text{Sr}$ ) to define groundwater processes occurring in a deep-seated landslide in flysch. *Hydrogeol. J.* 26 (8), 2669–2691.
- Durante, C., Baschieri, C., Bertacchini, L., Bertelli, D., Cocchi, M., Marchetti, A., Manzini, D., Papotti, G., Sighinolfi, S., 2015. An analytical approach to Sr isotope ratio determination in Lambrusco wines for geographical traceability purposes. *Food Chem.* 173, 557–563.
- Durante, C., Bertacchini, L., Cocchi, M., Manzini, D., Marchetti, A., Rossi, M.C., Sighinolfi, S., Tassi, L., 2018. Development of  $^{87}\text{Sr}/^{86}\text{Sr}$  maps as targeted strategy to support wine quality. *Food Chem.* 255, 139–146.
- Efremov, J.A., 1940. Taphonomy: new branch of paleontology. *Pan. Am. Geol.* 74 (2), 81–93.
- Enzo, S., Bazzoni, M., Mazzarello, V., Piga, G., Bandiera, P., Melis, P., 2007. A study by thermal treatment and X-ray powder diffraction on burnt fragmented bones from tombs II, IV and IX belonging to the hypogeic necropolis of “Sa Figù” near Ittiri, Sassari (Sardinia, Italy). *J. Archaeol. Sci.* 34, 1731–1737.
- Esposito, C., Gigante, M., Lugli, F., Miranda, P., Cavazzuti, C., Sperduti, A., Pacciarelli, M., Stoddart, S., Reimer, P., Malone, C., Bondioli, L., Müller, W., 2023. Intense community dynamics in the pre-Roman frontier site of Fermo (ninth-fifth century BCE, Marche, central Italy) inferred from isotopic data. *Sci. Rep.* 13, 36–132.
- Fahy, G.E., Deter, C., Pitfield, R., Miszkiewicz, J.J., Mahoney, P., 2017. Bone deep: Variation in stable isotope ratios and histomorphometric measurements of bone remodelling within adult humans. *J. Archaeol. Sci.* 87, 10–16.
- Faure, G., Mensing, T.M., 2005. *Isotopes: Principles and Applications*. Wiley.
- Faure, G., Powell, T., 1972. *Strontium Isotope Geology*. Springer, New York.
- Francisci, G., Micarelli, I., Iacumin, P., Castorina, F., Di Vincenzo, F., Di Matteo, M., Giostra, G., Manzi, G., Tafuri, M.A., 2020. Strontium and oxygen isotopes as indicators of Longobards mobility in Italy: an investigation at Povegliano Veronese. *Sci. Rep.* 10 (1), 1–12.
- Gerritzen, C.T., Goderis, S., James, H.F., Snoeck, C., 2024. Optimizing Zr-doped MC-ICP-MS sample-standard bracketing to simultaneously determine  $^{87}\text{Sr}/^{86}\text{Sr}$  and  $\delta^{88}\text{Sr}$  for high sample-throughput. *Spectrosc. Acta B* at Spectrosc. 217, 106955.
- Gonçalves, D., Cunha, E., Thompson, T.J.U., 2013. Weight references for burned human skeletal remains from portuguese samples. *J. Forensic Sci.* 58, 1134–1140.
- Gosman, J.H., Hubbell, Z.R., Shaw, C.N., Ryan, T.M., 2013. Development of Cortical Bone Geometry in the Human Femoral and Tibial Diaphysis. *Anat. Rec.* 296, 774–787.
- Harvig, L., Frei, K.M., Price, T.D., Lynnerup, N., 2014. Strontium isotope signals in cremated petrous portions as indicator for childhood origin. *PLoS One* 9, 101603.
- Higgins, O.A., Vazzana, A., Scalise, L.M., Riso, F.M., Buti, L., Conti, S., Bortolini, E., Oxilia, G., Benazzi, S., 2020. Comparing traditional and virtual approaches in the micro-excavation and analysis of cremated remains. *J. Archaeol. Sci. Rep.* 32, 102396.
- ICRP. 1973. *Alkaline Earth Metabolism in Adult Man*. In “A Report prepared by a task group of Committee 2 of the International Commission on Radiological Protection”. Edited by: Marshall, J. H., J. Limiecki, E. L. Lloyd, G. Marotti, C. W. Mays, J. Rundo, H. A. Sissons and W. S. Snyder. Oxford: The International Commission on Radiological Protection.
- Jörkov, M.L.S., Heinemeier, J., Lynnerup, N., 2009. The petrous bone - A new sampling site for identifying early dietary patterns in stable isotopic studies. *Am. J. Phys. Anthropol.* 139–199.
- Katsimbri, P., 2017. The biology of normal bone remodelling. *Eur. J. Cancer Care* 26, e12740.
- Kenkre, J., Bassett, J., 2018. The bone remodelling cycle. *Annals of Clinical Biochemistry: International Journal of Laboratory Medicine.* 55 (3), 308–327.
- Kerley, E.R., 1965. The microscopic determination of age in human bone. *American Journal of Biological Anthropology.* 23 (2), 149–163.
- Kovacs, C.S., 2016. Maternal Mineral and Bone Metabolism During Pregnancy, Lactation, and Post-Weaning Recovery. *Physiol. Rev.* 96, 449–547.
- Lightfoot, E., O'Connell, T., 2016. On the use of biomineral oxygen isotope data to identify human migrants in the archaeological record: intra-sample variation, statistical methods and geographical considerations. *PLoS One* 11, e0153850.
- Lugli, F., Cipriani, A., Tavaglione, V., Traversari, M., Benazzi, S., 2018. Transhumance pastoralism of Roccapelago (Modena, Italy) early-modern individuals: Inferences from Sr isotopes of hair strands. *Am. J. Phys. Anthropol.* 167 (3), 470–483.
- Lugli, F., Cipriani, A., Bruno, L., Ronchetti, F., Cavazzuti, C., Benazzi, S., 2022. A strontium isoscape of Italy for provenance studies. *Chem. Geol.* 587, 102624.
- Ma, C., Vander Zanden, H.B., Wunder, M.B., Bowen, G.J., 2020. assignR: an R package for isotope based geographic assignment. *Methods Ecol. Evol.* 11, 996–1001.
- Marchina, C., Natali, C., Fahnstock, M.F., Pennisi, M., Bryce, J., Bianchini, G., 2018. Strontium isotopic composition of the Po river dissolved load: Insights into rock weathering in Northern Italy. *Appl. Geochem.* 97, 187–196.
- Martin, J.T., Seeman, E., 2008. Bone remodelling: its local regulation and the emergence of bone fragility. *Best Pract. Res. Clin. Endocrinol. Metab.* 22 (5), 701–722.
- McKinley, J.L., 1994. Bone fragment size in British cremation burials and its implications for pyre technology and ritual. *J. Archaeol. Sci.* 21, 339–342.
- McMillan, R., Snoeck, C., Winter, N., Claeys, P., Weis, D., 2019. Evaluating the impact of acetic acid chemical pre-treatment on ‘old’ and cremated bone with the ‘Perio-spot’ technique and ‘Perios-endos’ profiles. *Palaeogeogr. Palaeoclimatol. Palaeoecol.* 530, 330–344.
- Nanci, A., 2003. *Ten Cate's Oral Histology: Development, Structure and Function*. Mosby, St Louis, MO.
- Noy, D., 2000. Building a Roman Funeral Pyre. *Antichthon* 34, 30–45.
- Ortalli, J., 2017. *Mutina*: Lo Spazio Funerario. In: Malnati, L., Pellegrini, S., Piccinini, F., Stefani, C. (Eds.), *Mutina* Splendidissima, La Città Romana e La Sua Identità. De Luca Editori D'Arte, Roma, pp. 166–206.
- Ortalli, J., 2011. Culto e riti funerari dei Romani: la documentazione archeologica. In: *Thesaurus Cultus et Rituum Antiquorum*. VI, pp. 198–215.
- Ortner, D.J., 2003. Identification of Pathological Conditions in Human Skeletal Remains, Identification of Pathological Conditions in Human Skeletal Remains. Elsevier Inc.
- Parfitt, A.M., 2013. Skeletal Heterogeneity and the Purposes of Bone Remodeling: Implications for the Understanding of Osteoporosis. In: Marcus, R., Feldman, D., Dempster, D.W., Luckey, M., Cauley, J.A. (Eds.), *Osteoporosis*, 4th ed. Academic Press, San Diego, pp. 855–872.
- Pellegrini, S., 2017. *Mutina*: La città. In: Malnati, L., Pellegrini, S., Piccinini, F., Stefani, C. (Eds.), *Mutina* Splendidissima, La Città Romana e La Sua Identità. De Luca Editori D'Arte, Roma, pp. 86–144.
- Person, A., 1995. Early Diagenetic Evolution of Bone Phosphate: An X-ray Diffractometry Analysis. *J. Archaeol. Sci.* 22, 211–221.
- Poletti Ecclesia, E., Tassinari, G., 2016. Archeologia della pietra ollare nel Verbano Cusio Ossola. Aree estrattive, segni di lavorazione, manufatti. In: Fantoni, R., Cerri, R., de Vingo, P. (Eds.), conference proceedings “La pietra ollare nelle Alpi. Coltivazione e utilizzo nelle zone di provenienza”.
- R Development Core Team, 2021. *R: A Language and Environment for Statistical Computing*. R Foundation for Statistical Computing, Vienna.
- Rottoli, M., Castiglioni, E., 2011. Plant offerings from Roman cremations in northern Italy: a review. *Veg. Hist. Archaeobotany* 20, 495–506.
- Salesse, K., Stamatakis, E., Kontopoulos, I., Verly, G., Annaert, R., Boudin, M., Capuzzo, G., Claeys, P., Dalle, S., Hlad, M., de Mulder, G., Sabaux, C., Sengeløv, A., Veselka, B., Warmenbol, E., Vercauteren, M., Snoeck, C., 2021. These boots are made for burnin': Inferring the position of the corpse and the presence of leather footwear during cremation through isotope ( $\delta^{13}\text{C}$ ,  $\delta^{18}\text{O}$ ) and infrared (FTIR) analyses of experimentally burnt skeletal remains. *PLoS One* 16.
- Schmidt, C.W., Symes, S.A., 2015. *The Analysis of Burned Human Remains*, 2nd ed. Elsevier.
- Shipman, P., Foster, G., Schoeninger, M., 1984. Burnt bones and teeth: an experimental study of colour, morphology, crystal structure and shrinkage. *J. Archaeol. Sci.* 11, 307–325.
- Snoeck, C., Lee-Thorp, J.A., Schulting, R.J., 2014. From bone to ash: Compositional and structural studies of burned bone. *Palaeogeogr. Palaeoclimatol. Palaeoecol.* 416, 55–68.
- Snoeck, C., Lee-Thorp, J.A., Schulting, R.J., de Jong, J., Debouge, W., Mattioli, N., 2015. Calcined bone provides a reliable substrate for strontium isotope ratios as shown by an enrichment experiment. *Rapid Commun. Mass Spectrom.* 29, 107–114.
- Stamatakis, E., Kontopoulos, I., Salesse, K., McMillan, R., Veselka, B., Sabaux, C., Annaert, R., Boudin, M., Capuzzo, G., Claeys, P., Dalle, S., Hlad, M., Sengeløv, A., Vercauteren, M., Warmenbol, E., Tys, D., De Mulder, G., Snoeck, C., 2021. Is it hot enough? A multi-proxy approach shows variations in cremation conditions during the Metal Ages in Belgium. *J. Archaeol. Sci.* 136.
- Surovell, T.A., Stiner, M.C., 2001. Standardizing Infra-red Measures of Bone Mineral Crystallinity: An Experimental Approach. *J. Archaeol. Sci.* 28, 633–642.
- Thompson, T.J.U., 2005. Heat-induced dimensional changes in bone and their consequences for forensic anthropology. *J. Forensic Sci.* 50, 185–193.
- Thompson, T.J.U., Gonçalves, D., Squires, K., Ulguim, P., 2017. Thermal Alteration to the Body. In: *Taphonomy of Human Remains: Forensic Analysis of the Dead and the Depositional Environment*. John Wiley & Sons Ltd., pp. 318–334.
- Van Strydonck, M., Boudin, M., De Mulder, G., 2010. The carbon origin of structural carbonate in bone apatite of cremated bones. *Radiocarbon* 52, 578–586.
- Veselka, B., Locher, H., de Groot, J., Davies, G.R., Snoeck, C., Kootker, L.M., 2021. Strontium isotope ratios related to childhood mobility: revisiting sampling strategies of the calcined human pars petrosa ossis temporalis. *Rapid Commun. Mass Spectrom.* 35 (7), e9038.
- Walker, P.L., Miller, K.W.P., Richman, R., 2008. Time, Temperature, and Oxygen Availability: An Experimental Study of the Effects of Environmental Conditions on the Color and Organic Content of Cremated Bone. *Elsevier Ltd.* 129–135.
- Weis, D., Kieffer, B., Maerschalk, C., Barling, J., de Jong, J., Williams, G.A., Hanano, D., Pretorius, W., Mattioli, N., Scoates, J.S., Goolaerts, G., Friedman, R.M., Mahoney, J.

- B., 2006. High-precision isotopic characterization of USGS reference materials by TIMS and MC-ICP-MS. *Geochem. Geophys. Geosyst.* 7.
- White, T., Folkens, P., 2012. *The Human Bone Manual*, the Human Bone Manual. Elsevier Inc.
- Williams, H., 2008. Towards an archaeology of cremation. In: Schmidt, C.W., Symes, S.A. (Eds.), *The Analysis of Burned Human Remains*. Academic Press, Amsterdam.
- Zazzo, A., Lebon, M., Chiotti, L., Comby, C., Delqué-Kolic, E., Nespoulet, R., Reiche, I., 2013. Can we Use Calcined Bones for  $^{14}\text{C}$  Dating the Paleolithic? *Radiocarbon* 55 (3), 1409–1421.